PACKER ENGINEERING INC,
1950 North Washington Street,
Naperville, IL 60566

Metallurgical Evaluation of a Nurse Tank Cracked Head

Final REPORT

April 26, 2008

Prepared for
Mark Toughiry
Office of Hazardous Materials Technology
Pipeline and Hazardous
Materials Safety Administration
U.S. Department of Transportation

Purchase Order No. DAS - 438

Table of Contents

Metallurgical Evaluation of a Nurse Tank Cracked Head

1.0 INTRODUCTION

Objective: - The purpose of this project is to analyze a ruptured 1000 gallon NH_3 tank to determine the crack initiation site (CIS) and the cause of the tank failure.

1.1 Background

On 11/21/2007 it was reported that, "a nurse tank carrying anhydrous ammonia exploded and pieces were found laying in the front yard of a farm just outside of Silver Lake, Minnesota. The driver was taken to the hospital due to exposure to the NH_3." The incident occurred near Kale Avenue (McLeod County 90), just south of MTH 7. A scene investigation revealed the tank had torn off its running gear, impacted the back of the pick-up truck (tow vehicle) and then was propelled across the front yard of a farm. All the NH_3 had been expelled from the 1000 gallon capacity tank and dissipated. The tank is owned by Crop Production Services, Inc (CPS), (DOT # 300176).

1.2 Technical Approach

The ruptured nurse tank head was analyzed to determine the cause and origin of the tank head rupture.

Upon arrival at Packer Engineering (Packer), the general condition of the tank head was documented. All markings on the tank surface were identified and recorded. The cylinder was then cut open to analyze the fracture surfaces. Using oblique lighting, the suspected fracture initiation site was identified during visual examination of the fracture surface. Replica strips were used to remove loose deposits from the fracture surface near the suspected origin. The fracture surface was then removed from the tank head by band saw sectioning. The fracture surface was cleaned a second time in a solution containing 20% methanol + 40% acetone + 40% toluene.

To determine the fracture mode, the cleaned fracture was analyzed using both a low powered stereomicroscope and a scanning electron microscope (SEM). A chemical analysis was also performed on a representative sample taken near the fracture surface. Rockwell hardness test, tensile tests, fracture toughness test and Charpy impact tests were performed to evaluate the mechanical properties of the tank head material.

2.0 GENERAL DOCUMENTATION OF THE TANK

2.1 Visual Documentation and Cylinder Specifications

Tank Information

- The subject tank was identified with serial # 171843 and was manufactured in 1973. Figure 1 shows the ruptured tank.
- Nurse tank nameplate data was identified by the Crop Production Services, Dassel, MN facility as #17.
- Tank was manufactured by Chemtrol Chemical Co. of Fremont, Ohio.
- Tank length: 192 inches.
- Tank diameter : 40.5 inches.
- Square foot area: 132 sq ft.
- Head metal thickness: 0.230 inch.
- Shell metal thickness: 0.321 inch.
- Design/Working pressure or MAWP: 250 psig @ 650 degrees Fahrenheit.
- ASME Construction Code Symbol Stamps: U, W, PRT, Div 1, Stressed relieved heads. Inspection stamp: "CU" (suspect Commercial Union).
  U - Vessel inspected in accordance with UG-90 through UG-97.
  W – Arc or gas welded.
  PRT – Part of the vessel has been radiographed.
  Div 1: in compliance with ASME section VIII pressure vessels division 1.
- Gallon capacity: 992 gallons.

Visual Examination Details

- Packer Engineering received the tank head shown in Figures 2 and 3. The tank head is labeled as anhydrous ammonia UN 1005.
- The location of the rupture on the tank head is shown in Figure 2.
- Figure 4 shows the inside surface of the tank head.
- Two additional cracks were observed on the inside surface of the tank head as shown in Figure 5.
- There are signs of impact damage to one side of the tank head and the paint has been removed as shown in Figure 6.
- There was corrosion found in one area of the tank head where paint had peeled off. This corrosion is shown in Figure 7.

3. METALLURGICAL ANALYSIS

3.1 Visual Observation and Sectioning of the Cylinder

The tank head was cut at the locations shown in Figures 8 and 9 to expose the fracture surface for further analysis. The fracture surface was visually examined and the crack initiation site was identified. The fracture origin coincided with the edge of a large dent on the exterior of the tank head (Figure 6). Visual examination suggested this dent was present prior to the rupture and not caused during the catastrophic event as multiple scratch patterns were associated with the dent as shown in Figure 10.

The fracture surface near the origin was cleaned using replica strips to remove loose corrosion products from the surface. After the crack initiation site was confirmed, the area containing the origin was marked and sectioned, as shown in Figure 10, to perform fractography and optical microscopy.

3.2 Chemical Analysis of the Cylinder

The chemical composition of the subject tank head was determined by emission spectrography. Carbon and sulfur were determined by LECO combustion. The tank is made of carbon steel and the composition is similar to American Society of Testing Materials (ASTM) A285 carbon steel pressure vessel plate Grade C. The chemical composition of the tank material is shown in Table I. Also included in Table I are the chemical requirements for ASTM A285 carbon steel, Grade C for comparison. ASTM A285 is an approved material for pressure vessel construction per American Society of Mechanical Engineers (ASME) Boiler and Pressure Vessel Code Section VIII, 1971 Pressure Vessels Division 1 [1].

Table I: Results of chemical composition, weight %.

Elements	Tank Head	ASTM A285, Grade C
Carbon (C)	0.22	0.28 Max
Manganese (Mn)	0.54	0.90 Max
Phosphorus (P)	<0.005	0.035 Max
Sulfur (S)	0.015	0.045 Max
Silicon (Si)	<0.01	-
Chromium (Cr)	0.01	0.25 Max
Nickel (Ni)	0.04	0.25 Max
Molybdenum (Mo)	<0.01	0.08 Max
Copper (Cu)	0.02	0.035 Max
Aluminum (Al)	<0.005	-

3.3 Fractography and Metallography

The fracture surface at the fracture origin can be seen in Figure 11. The fracture surface at location "A" and "B" in Figure 10 can be seen in Figures 12 and 13, respectively. The fracture surface has an appearance characteristic of brittle, faceted fracture.

The removed portion of the fracture was also observed under a stereomicroscope at magnifications up to 60X. Figures 14 and 15 are stereoscope images detailing the fracture appearance at the fracture origin. The fracture surface is faceted which is consistent with brittle fracture. Additionally, no shear lip and/or plastic deformation was evident which is also characteristic of brittle fracture.

The fracture surface was then ultrasonically cleaned in a methanol-acetone-toluene solution and analyzed using a scanning electron microscope (SEM). The SEM images can be seen in Figures 16 - 20. SEM analysis confirmed brittle fracture at and away from the fracture origin. Transgranular cleavage and intergranular fracture were observed. Figures 17, 19 and 20 are SEM fractograph images showing the transgranular cleavage and intergranular fracture observed during SEM examination.

As shown in Figure 21, two additional cracks were observed on the ID of the tank running parallel to the fracture surface. These two cracks were not through-thickness cracks as no cracking was observed on the tank OD. Figure 22 shows the absence of cracking on the tank OD at the location of the two ID cracks. For identification purposes, these two cracks were identified as Crack 1 and Crack 2. Figure 21 illustrates how the cracks were identified.

A metallographic section was prepared through both Crack 1 and Crack 2 by sectioning the tank transversely near the end of the cracks. The metallurgical mount was polished and etched with 2% Nital solution. Figures 23 - 25 show the microstructure and profile of Crack 1 at the ID of the tank. The figures show a typical ferrite/pearlite microstructure with decarburization along the ID of the tank. Crack 1 was both transgranular and intergranular at the ID surface of the tank.

Figures 26 to 28 show the microstructure and profile of Crack 1 near the crack tip (arrest point). As evident in the figures, Crack 1 exhibited significant crack branching near the crack tip. The microstructure was consistent with carbon steel as equiaxed ferrite/pearlite grains were observed.

Figures 29 - 31 show the microstructure and profile of Crack 2 at the ID of the tank. The figures show a typical ferrite/pearlite microstructure with decarburization along the ID of the tank. Crack 2 was both transgranular and intergranular at the ID surface of the tank.

Figure 32 - 34 show the microstructure and profile of Crack 2 near the crack tip (arrest point). As evident in the figures, Crack 2 exhibited significant crack branching near the

crack tip. The microstructure was consistent carbon steel as equiaxed ferrite/pearlite grains were observed.

The cross section revealed the cracks tended to propagate through the thickness of the tank in both a transgranular and intergranular mode. Considerable crack branching and/or secondary cracking was also present and both cracks were found to initiate on the ID of the tank.

4 MECHANICAL PROPERTY EVALUATION

Samples for Rockwell hardness testing, tensile testing, fracture toughness testing and impact tests were obtained from the area shown in Figure 35.

4.1 Rockwell Hardness:

Rockwell hardness testing was performed on the tank head steel in accordance with ASTM E18-98. The results of the Rockwell hardness testing are shown in Table II.

Table II: Rockwell Hardness Data (HRB).

Location	Hardness (HRB)
1	88
2	88
3	89
4	88
5	88
Average	88

4.2 Tensile Test

Two tensile samples were prepared from representative samples to determine the strength and elongation. The tensile results are presented in Table III.

Table III: Tensile Results.

Property	Sample 1	Sample 2
Yield Strength (ksi)	**62.9**	**61.9**
Tensile Strength (ksi)	**69.6**	**72.3**
Elongation (%)	**16.3 %**	**14.5 %**

4.3 Fracture Toughness Test

Compact type specimens were prepared from the tank head in a manner to maximize the thickness of the specimen. The tests were conducted at ambient temperature.

The J-Integral tests results did not produce a valid J_{IC} value for either sample as neither sample displayed unstable crack extension. The values of J_{Qc}, the maximum value of J prior to instability are shown in Table IV.

The samples were then evaluated for plain strain fracture toughness criteria. The P_{max} and P_q values and ratios are shown in Table IV for both samples. The values of K_q are also presented in Table IV. A valid K_{IC} requires the ratio of P_{max} to P_q be less than 1.1 and the test specimen thickness to be greater than $2.5(K_q/YS)^2$. As evident from the Table, neither specimen met the requirements for a valid K_{IC} test.

Therefore, due to the size (thickness) and strength (yield strength) of the tank head, Packer could not obtain valid K_{IC} or J_C test data. The testing did show that both samples exhibited unstable crack extension. This test data confirms the finding that the tank head steel is brittle and susceptible to rapid catastrophic fracture.

Table IV: Results of J-integral tests

Parameter	Sample 1	Sample 2
B, Bn	0.205 in	0.203 in
W	1.011 in	1.011 in
Aoq	0.4732 in	0.5671 in
Afq	0.4933 in	0.5821 in
ΔK_f	24.5 ksi-in$^{1/2}$	33.05 ksi-in$^{1/2}$
Displacement Control, rate	0.000334 in/sec.	0.000334 in/sec
J_{Qc}	114.5 lbf/in	218.9 lbf/in.
Pmax	1116 lbf	916 lbf
Pq	803 lbf	638 lbf
Pmax/Pq	1.39	1.44
Kq	36.3 ksi-in$^{1/2}$	38.9 ksi-in$^{1/2}$
$2.5(kq/YS)^2$	0.845 in	0.973
Fracture appearance	Brittle, no subcritical crack growth	Brittle, no subcritical crack growth

4.4 Impact Test

Impact Charpy impact test was performed on two specimens at -20ºF. The size of the Charpy V-notch type was 10mm x 5mm taken in accordance with ASTM A370-77. The fracture toughness of both samples tested was < 1 ft-lbs at -20°F.

5 DISCUSSION

A metallurgical evaluation was performed on the tank head with serial number 171843 to identify the cause and origin of the tank rupture. During the investigation, it was found that the fracture origin was located on the ID of the tank at the side of the tank head shown by the arrow in Figure 6. The OD of the tank at this location was damaged (dented) due to contact with a foreign object. Based upon the scratch patterns, Packer suspects this dent was pre-existing and not created during the rupture event. The fracture origin was associated with the edge of this dent on the ID surface of the tank.

Examination of the fracture surface revealed brittle transgranular and intergrannular fracture. No evidence of plastic deformation was visible. Two additional cracks, which were parallel to the fracture, were present beneath the fracture surface. Both of these cracks were pre-existing (prior to final fracture) as fracture intersected both of these cracks. A metallurgical cross section prepared through these cracks revealed extensive crack branching as well as a transgranular and intergranular fracture mode. This crack propagation mode is identical to the intergranular and transgranular cleavage fracture observed during SEM examination of the fracture surface. Extensive crack branching and brittle fracture are consistent with stress corrosion cracking (SCC).

The subject nurse tank is made of carbon steel and was used for transportation of anhydrous ammonia. Nurse tanks made of carbon steel are susceptible to SCC in an anhydrous ammonia environment [2-8].

According to the American Society for Metals "Metals handbook, intergranular fracture in carbon steel in presence of a caustic material such as anhydrous ammonia is typical of stress- corrosion cracking. [7] Research also indicates that SCC of mild steel in liquid and anhydrous ammonia can have transgranular mode of failure [8]. This supports the fact that the SCC propagated by both intergranular and transgranular modes in the presence of anhydrous ammonia.

SCC requires - (1) a susceptible material, (2) exposure to a particular environment and (3) tensile stresses. Based on all the research done to identify the cause of SCC of carbon steel in anhydrous ammonia environments, the following have been identified as possible causes:

(1) Residual stresses from the forming and manufacturing process. To minimize the susceptibility to SCC, pressure vessels should be either fully stress relieved or fabricated with heads that are hot formed or stress relieved [3], [4], [6].

(2) SCC initiation requires oxygen [2]. Extreme care should be used to eliminate air from the ammonia system. New vessels must be purged to eliminate air contamination [3] [4]. Contamination of air is the primary cause of SCC in ammonia [5].

(3) Ammonia should contain at least 0.2% water to inhibit SCC [3], [4], [6]

(3) SCC increases with increasing stress levels and increasing yield strength of the plate material [2-5] [7].

(4)

In the present case, high residual stresses may have been generated due to the dent on the exterior (OD) of the tank. The residual tensile stresses generated by this dent made the tank susceptible to SCC.

Packer has no information on the service life and the water content of the anhydrous ammonia stored in the subject tank. Air contamination and/or transporting anhydrous ammonia with low water content could have been a contributing factor. However, no information has been provided to Packer that indicates the subject nurse tank was contaminated with air or transported anhydrous ammonia with low water content.

The mechanical testing revealed the subject tank has low Charpy impact toughness properties. Additionally, fracture toughness testing revealed the subject vessel is nOT flaw tolerant and does not satisfy "leak before break" criteria. A higher toughness steel would have allowed a through wall crack to develop in the tank without resulting in rapid fracture. The through wall crack would have allowed anhydrous ammonia to "leak" from the tank versus causing a rapid fracture at normal operating pressures. The low toughness of the tank head steel resulted in the catastrophic failure of the vessel.

The cause for the low toughness is unknown, but may be the result of strain age embrittlement. The steel utilized to manufacturer the vessel may have had adequate toughness in 1973. However, aging (strain age embrittlement) could have severely degraded the toughness and ductility of the vessel. Additional testing would be necessary to determine the mechanism(s) which contributed to the tank's low toughness.

A similar type of anhydrous ammonia tank explosion was reported in June 6, 2005 at Morris in Minnesota. The tank was also built in 1973 and was also manufactured by Chemtrol Chemical Company and had the same dimensions and capacity as our subject tank. In that case, a small crack was seen on the inside surface of the vessel head [9].

6 CONCLUSIONS

1. Rupture of the subject tank head was due to SCC.

2. Residual stresses generated by the dent on the side of the tank's head most likely made the tank susceptible to SCC in anhydrous ammonia environment.

3. Charpy impact and fracture toughness testing indicate the tank is susceptible to brittle fracture. The brittleness of the steel may be the result of strain age embrittlement.

4. The chemical composition meets the requirement specified for ASTM A285.

This concludes Packer Engineering's report to date. If additional information becomes available, Packer Engineering will consider it and amend our report, if necessary. Should you have any questions, please contact Mridula Pareek at mpareek@packereng.com or call 630-577-1930.

Respectfully submitted,

PACKER ENGINEERING, INC.

Prepared by:

Mridula L Pareek
Engineering Technologist,
Technical Services

Reviewed by:

Kevin L Jones P.E.
Senior Staff Engineer,
Materials Engineering

7 FIGURES

Figure 1: The subject nurse tank in storage after the rupture.

Figure 2: The tank head received by Packer Engineering. The label indicates that it is used to transport anhydrous ammonia.

Figure 3: Shows the portion of the nurse tank received by Packer Engineering.

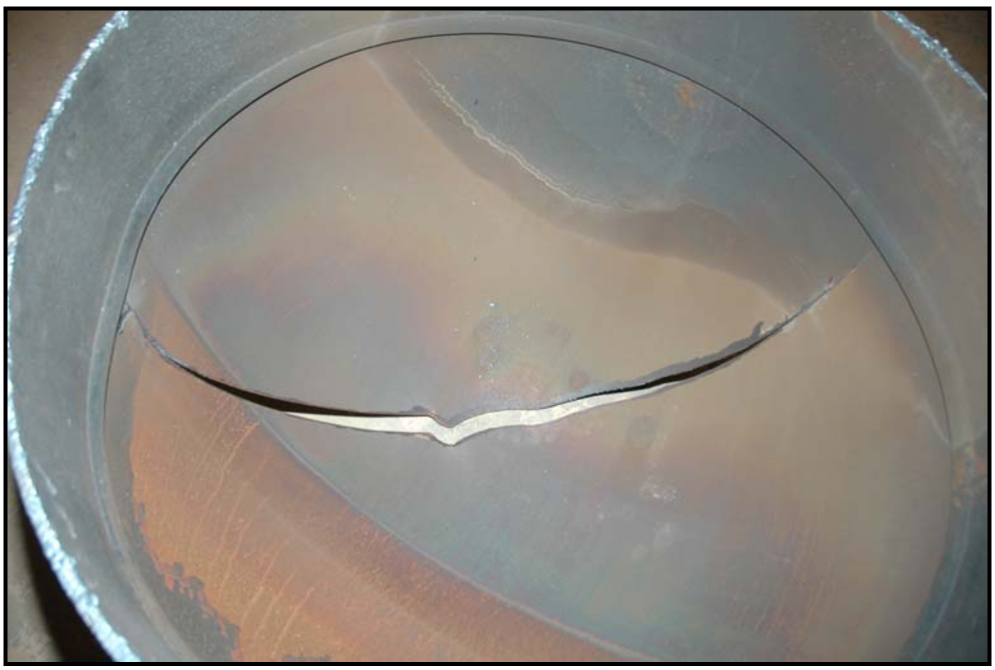

Figure 4: Shows the inside surface of the nurse tank head.

Figure 5: Two cracks (indicated by arrow) observed parallel to the fracture surface on the ID of the tank head.

Figure 6: Shows impact damage and peeling of paint on the tank head. Arrow indicates the location of the two cracks on the inside surface of the tank head.

Figure 7: Shows corrosion on the tank head.

Figure 8: Image shows where (red line) the tank was cut to expose the fracture surface.

Figure 9: Image shows where (red line) the tank was cut to expose the fracture surface.

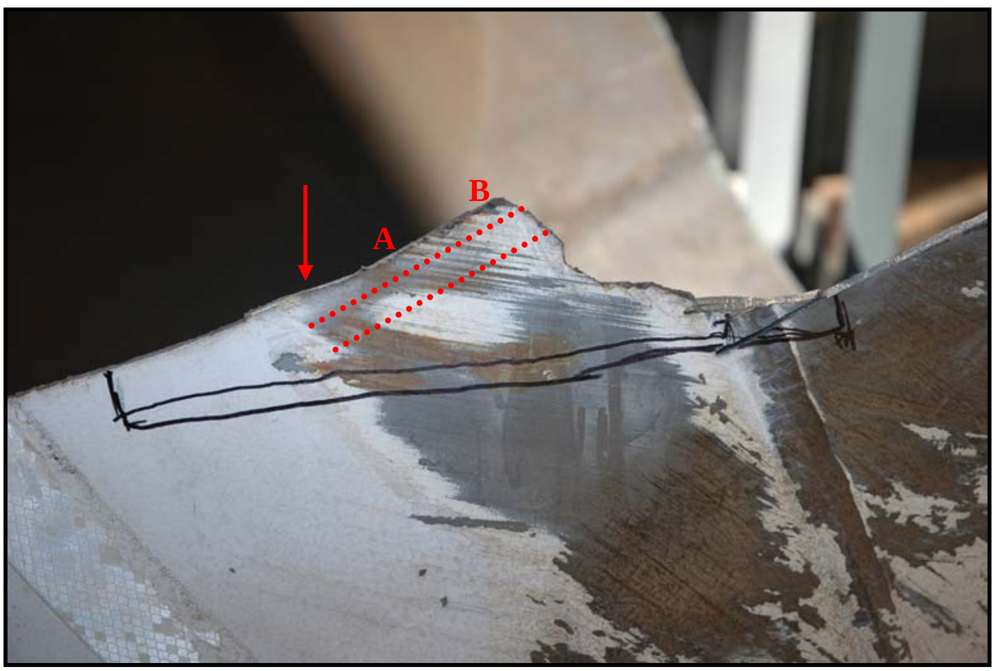

Figure 10: Shows area on the tank head containing the origin of the fracture (as indicated by arrow). There were two cracks found on the ID of the tank head running parallel to the fracture surface near origin. These two cracks are illustrated by the red dotted lines.

Figure 11: Photograph of the fracture surface at the fracture origin. A small, faint clamshell pattern was observed at the fracture origin. The fracture surface appears to be brittle and faceted.

Figure 12: Photograph of the fracture surface at location "A" identified in Figure 10.

Figure: 13 Photograph of the fracture surface at location "B" identified in Figure 10.

Figure 14: Stereoscope image at the fracture origin. The fracture surface at the origin appeared flat and faceted. A faint clam shell pattern was also observed at the fracture origin.

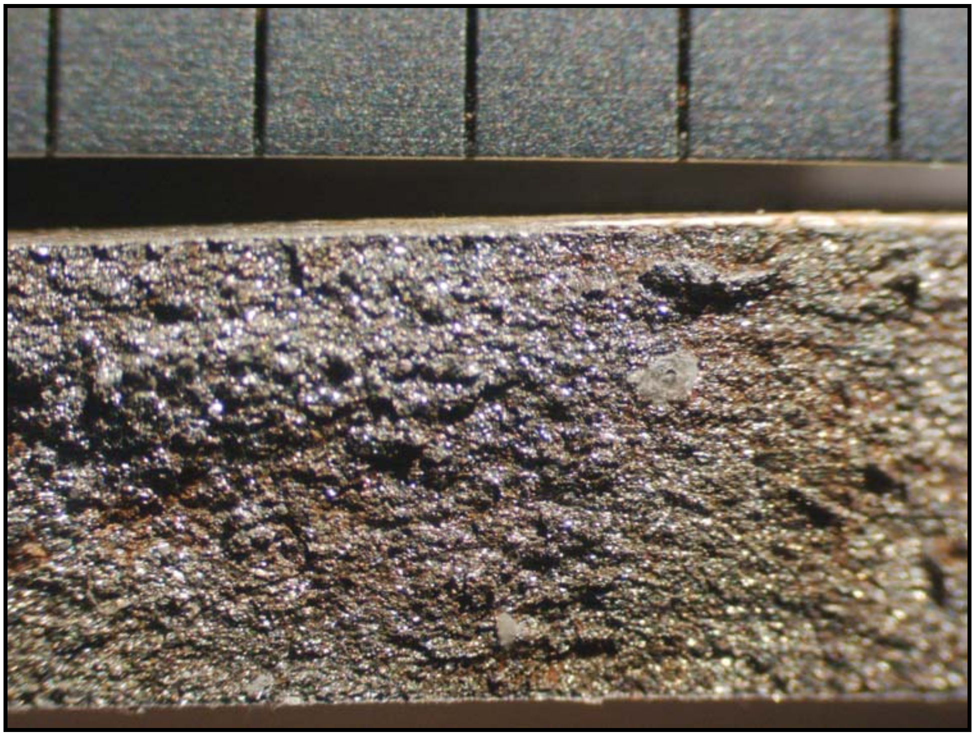

Figure 15: Stereoscope image of the fracture origin at higher magnification.

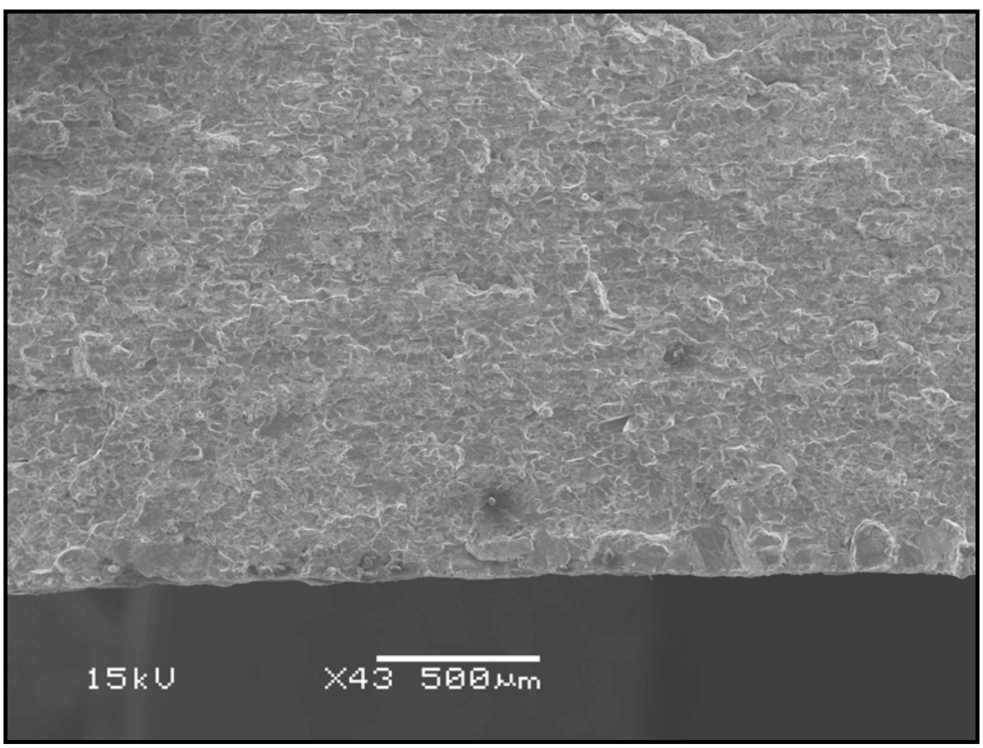

Figure 16: SEM image of the fracture surface at the origin.

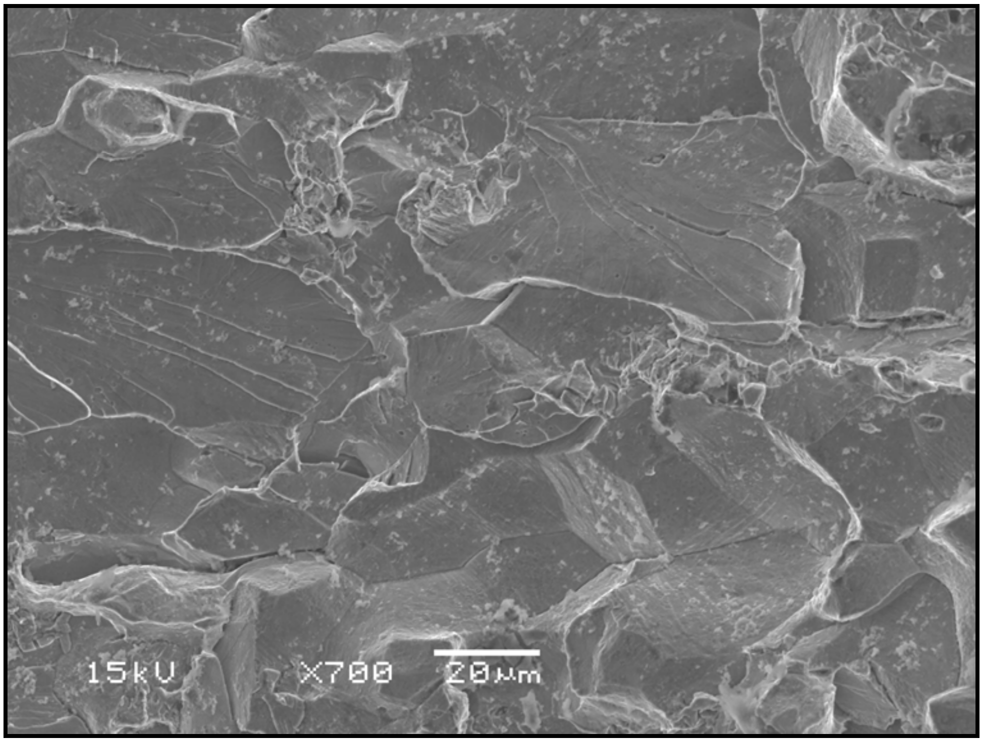

Figure 17: SEM image of the fracture surface at the origin at higher magnification. Both transgranular cleavage and intergranular fracture are evident in the figure.

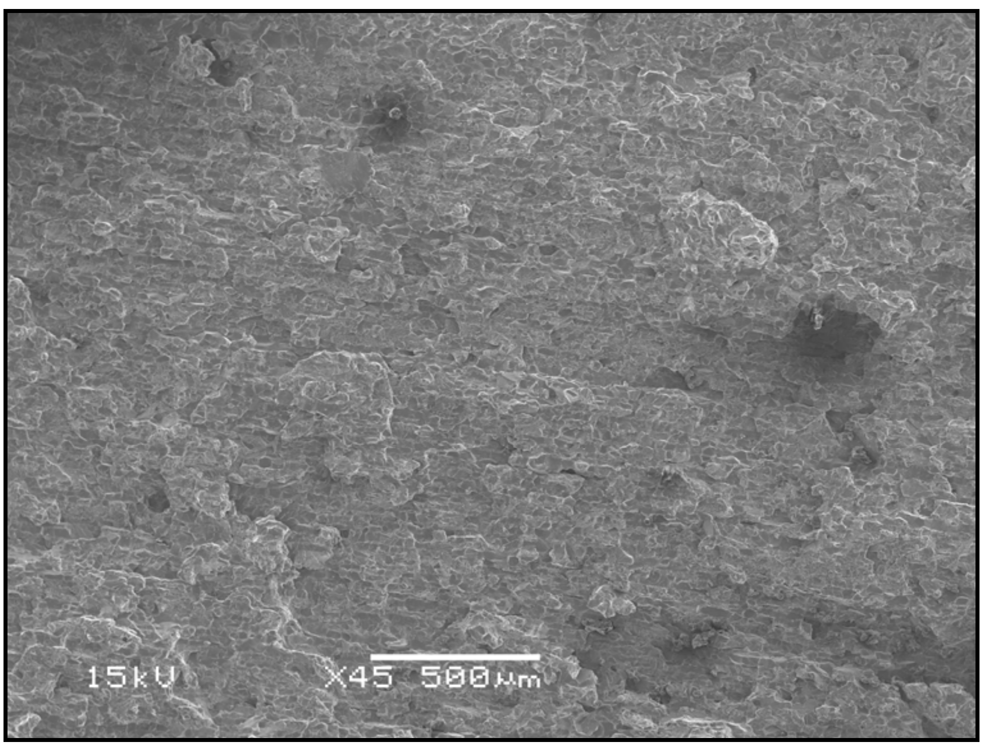

Figure 18: SEM image of the fracture surface away from the origin.

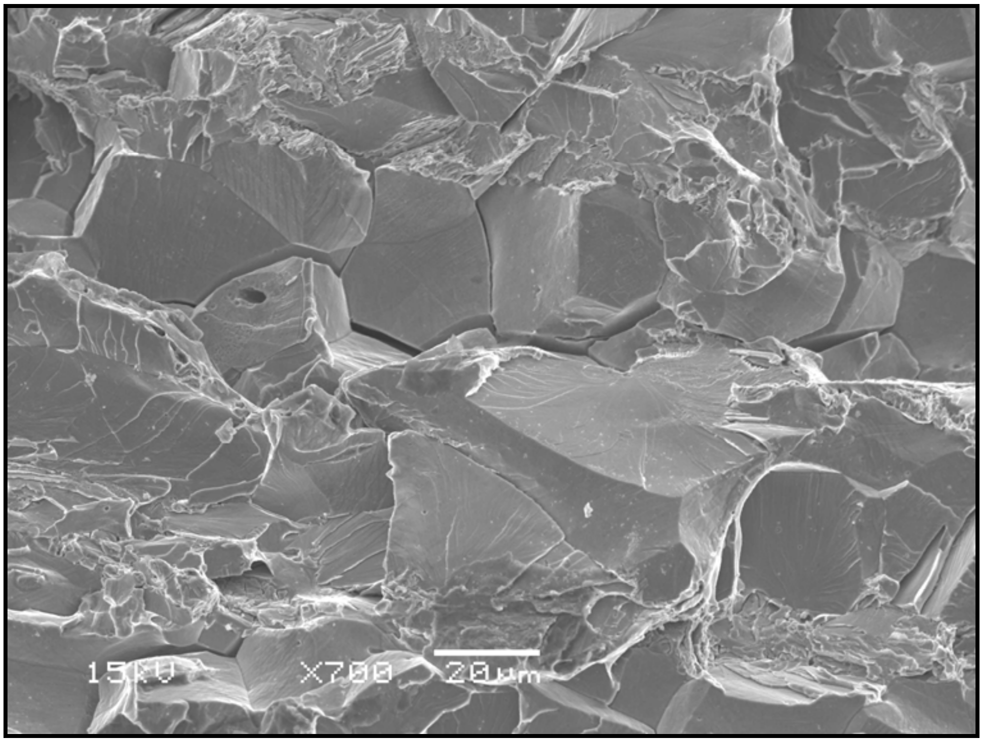

Figure 19: SEM image of the fracture surface away from the origin at higher magnification. Both transgranular cleavage and intergranular fracture are evident in the figure.

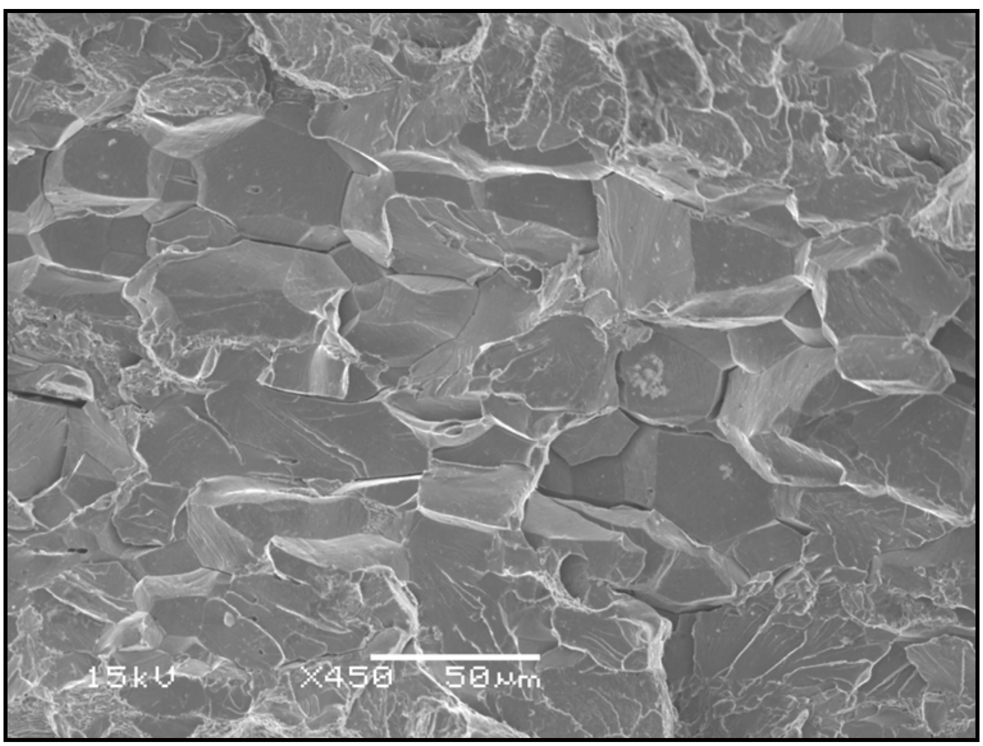

Figure 20: SEM image of the fracture surface away from the fracture origin. Both transgranular cleavage and intergranular fracture are evident in the figure.

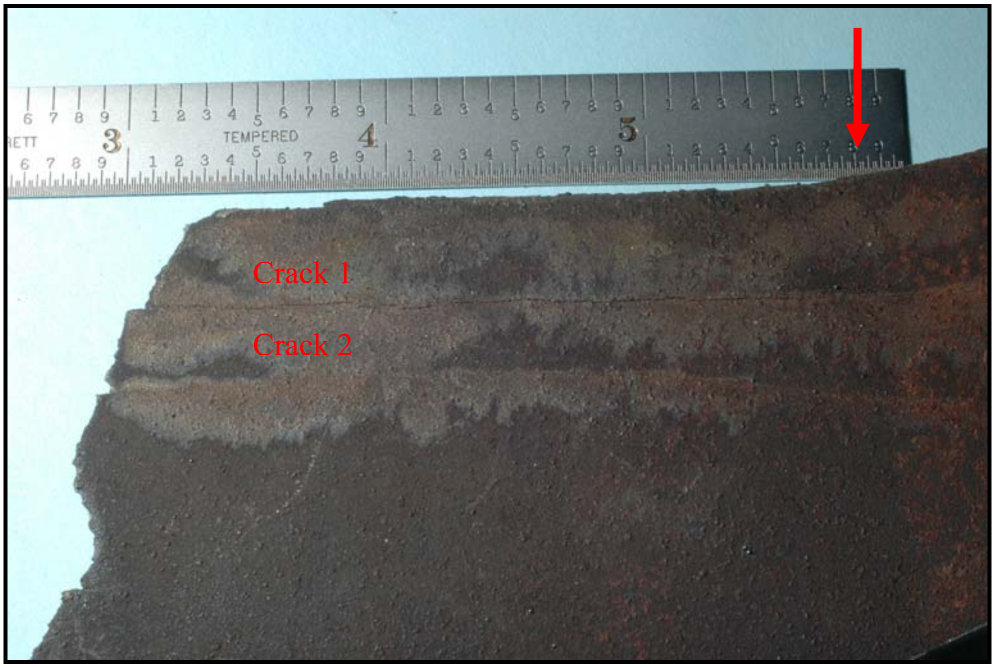

Figure 21: Shows the two cracks found on the inside surface of the tank head. Notice how the cracks run parallel to the fracture. Red arrow points to the approximate fracture origin.

Figure 22: Shows that the cracks on the inside surface have not extended to the outside surface of the tank head.

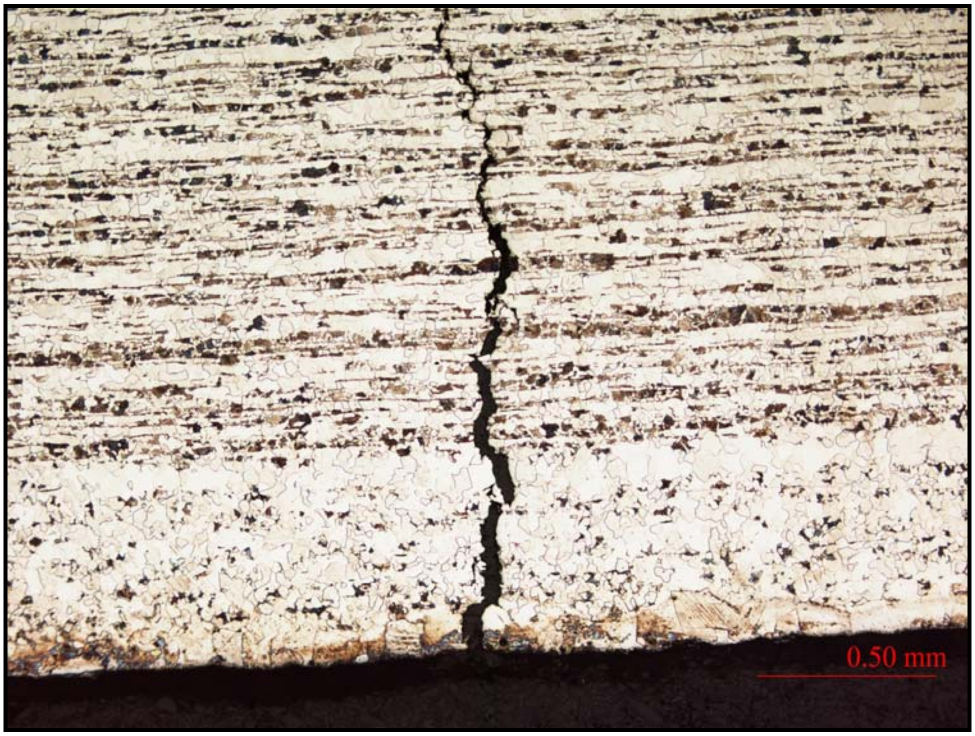

Figure 23: Metallograph image showing the ferrite/pearlite microstructure and the profile of Crack 1 at the ID of the tank. The steel is decarburized at the ID surface. Magnification: 50 X. Etchant: 2% Nital

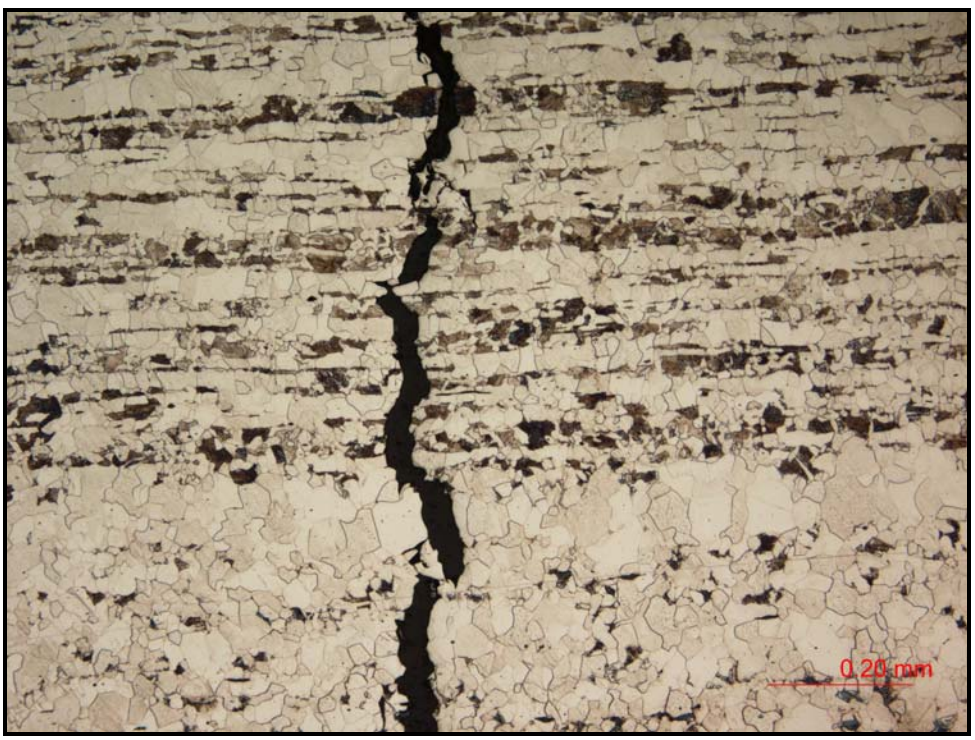

Figure 24: Same area as Figure 23 at higher magnification. Magnification: 100 X. Etchant: 2% Nital

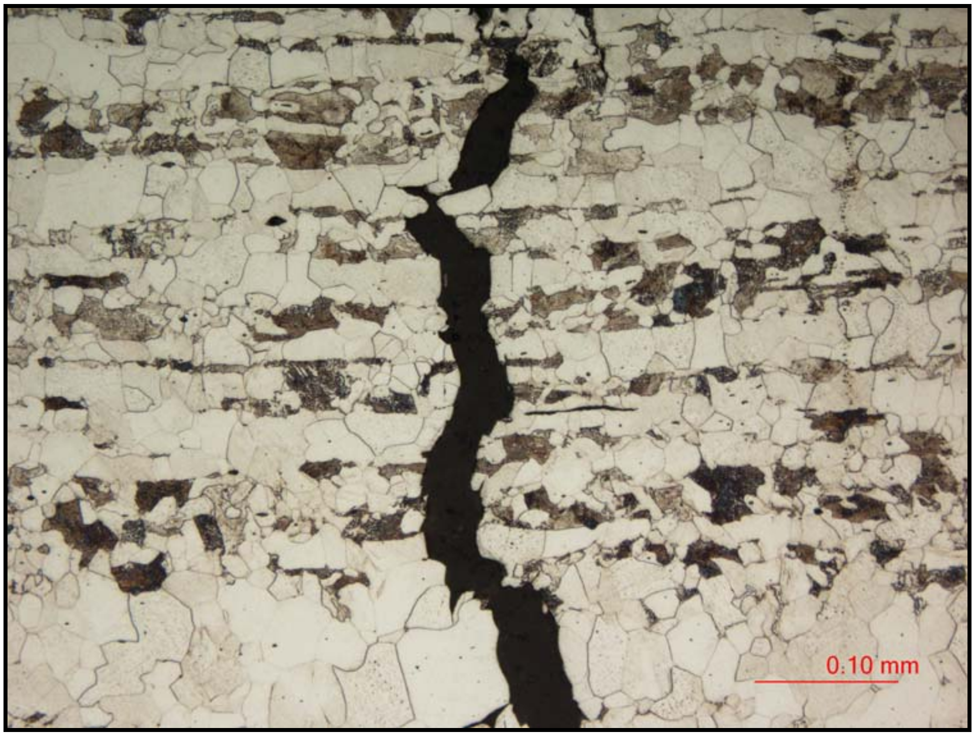

Figure 25: Same area as Figure 23 showing the trangranular and intergranular nature of the crack. Magnification: 200 X. Etchant: 2% Nital

Figure 26: Metallograph image showing the ferrite/pearlite microstructure at tip of Crack 1. Image also shows the general profile of Crack 1 at the crack tip. Magnification: 50 X. Etchant: 2% Nital

Figure 27: Same area as Figure 26 at higher magnification. Notice the crack branching at the crack tip. Magnification: 100 X. Etchant: 2% Nital

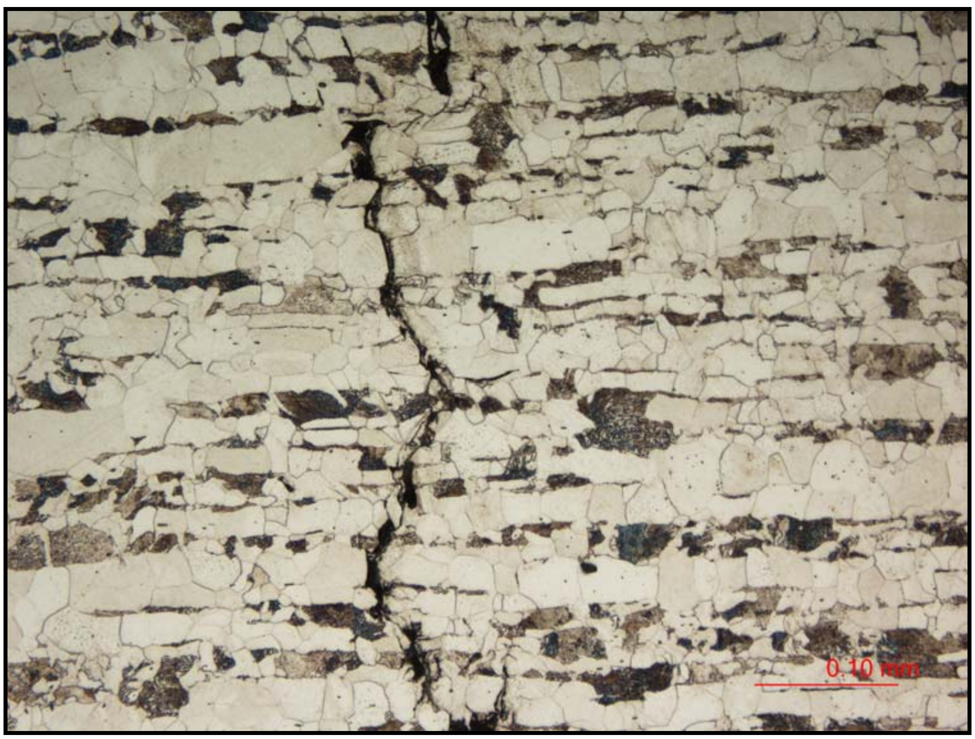

Figure 28: Same area as Figure 26 at higher magnification. Notice the crack branching at the crack tip. Both intergranular and transgranular crack propagation are evident in the figure. Magnification: 200 X. Etchant: 2% Nital.

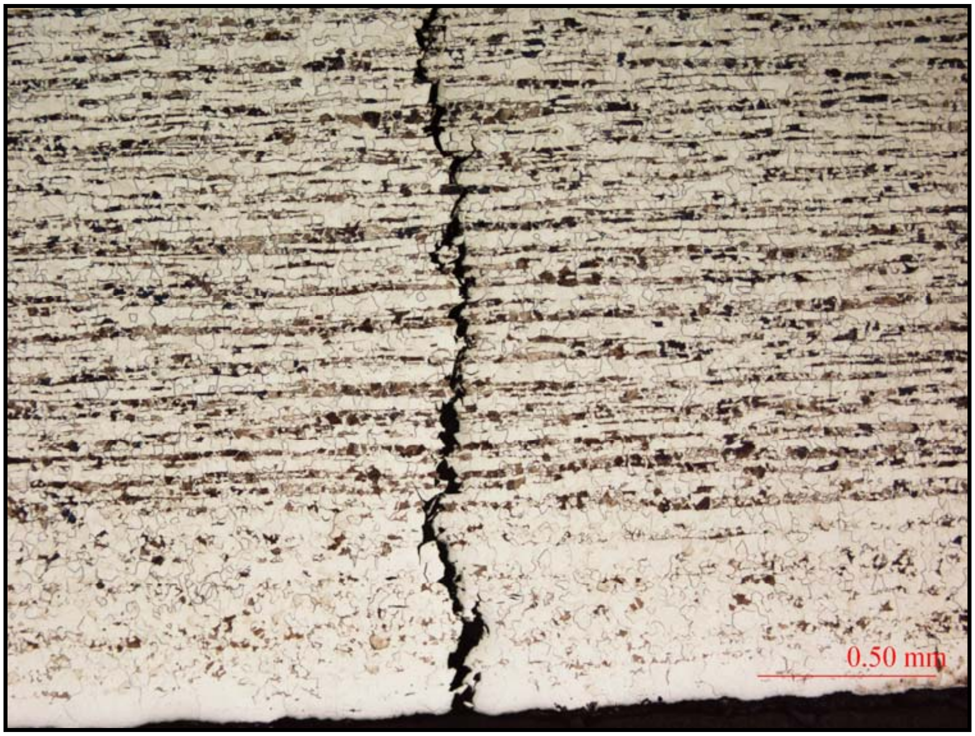

Figure 29: Shows the ferrite/pearlite microstructure and Crack 2 profile at the beginning of the cut section. Magnification: 50 X. Etchant: 2% Nital

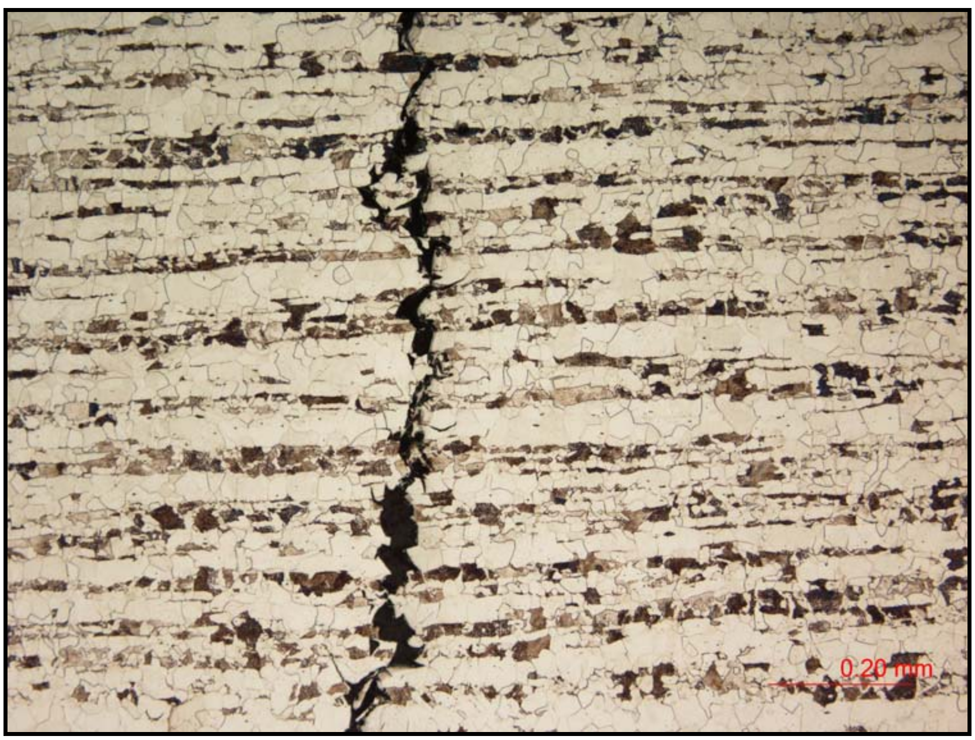

Figure 30: Same area as Figure 29 at higher magnification. Magnification: 100 X. Etchant: 2% Nital

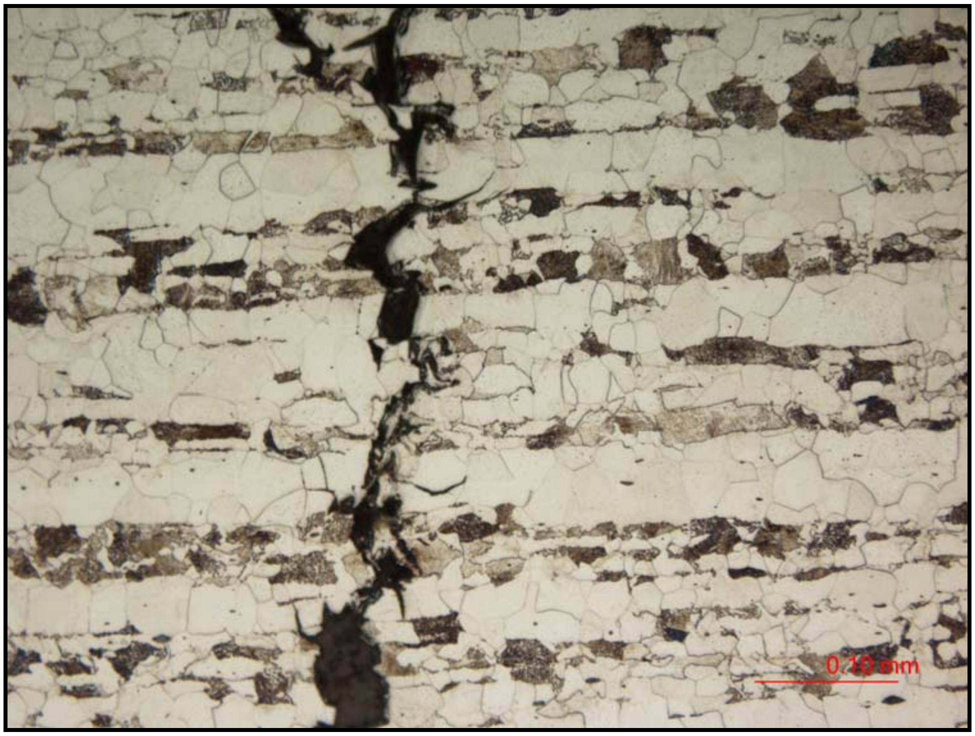

Figure 31: Same area as Figure 29 at higher magnification. The crack is trangranular and intergranular. Magnification: 200 X. Etchant: 2% Nital

Figure 32: Shows the ferrite/pearlite microstructure and Crack 2 profile at the end of the crack. Magnification: 50 X. Etchant: 2% Nital

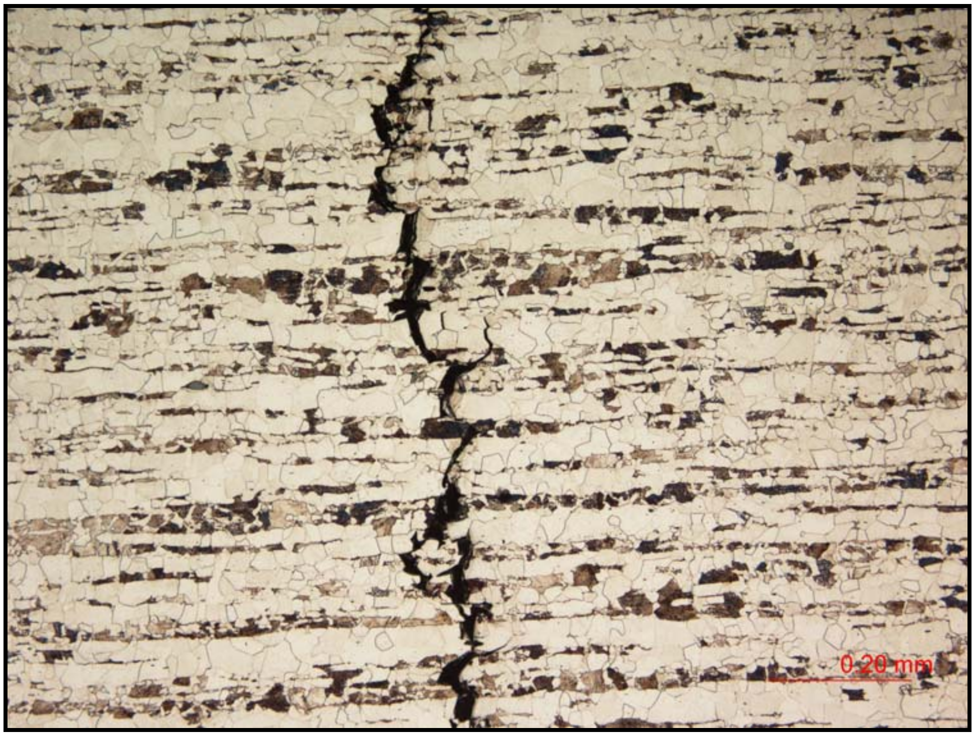

Figure 33: Same area as Figure 32 at higher magnification. Magnification: 100 X. Etchant: 2% Nital

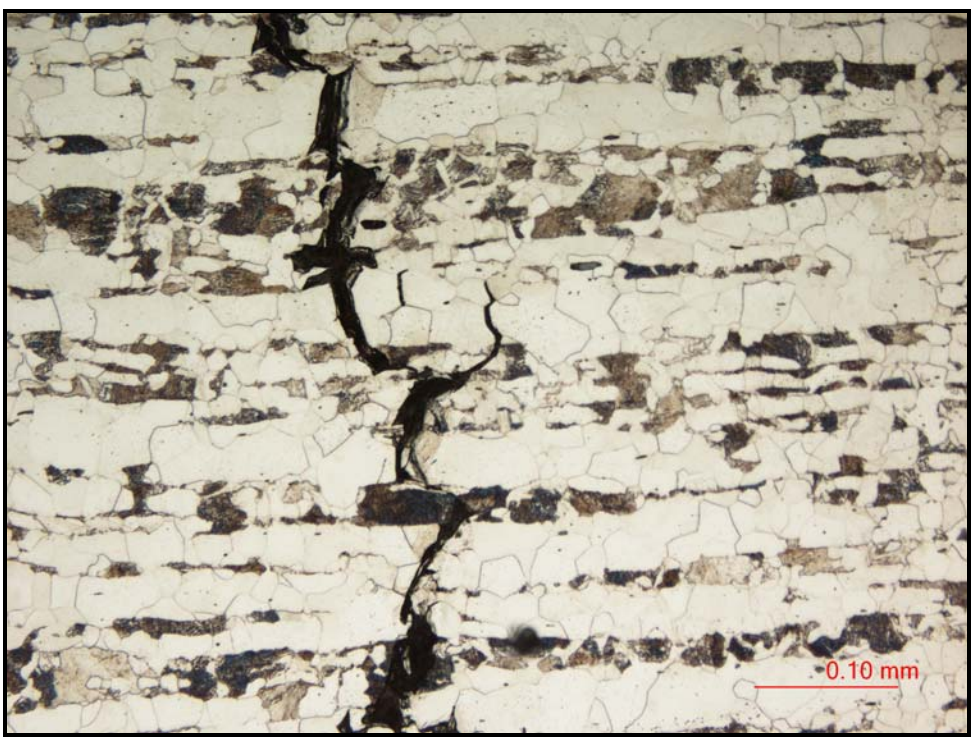

Figure 34: Same area as Figure 32 at higher magnification. The crack is trangranular and intergranular. Magnification: 200 X. Etchant: 2% Nital

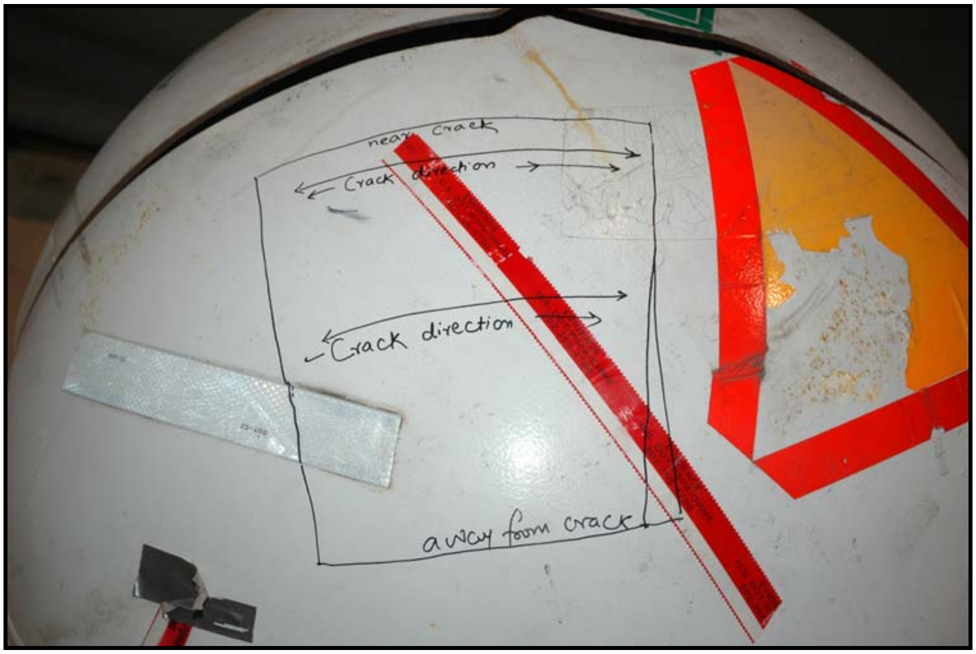

Figure 35: Shows the location on the tank head from where the samples were prepared for chemistry, hardness, tensile, impact and fracture toughness testing.

8. REFERENCES

1. ASME Boiler and pressure vessel code, Section VIII, pressure vessels, Division 1 (1971).
2. Guidance for inspection of atmospheric refrigerated ammonia storage tank second edition, EFMA – European fertilizer manufacturers association (2008).
3. “Stress corrosion cracking of steel in liquefied ammonia service – a recapitulation”, by A.W. Longinow (1989)
4. The Cold Front, Stress corrosion cracking prevention, Vol 5, No2, IRC Wisconsin (2005)
5. “Stress corrosion cracking of different steels in ammonia with special emphasis on vapour phase cracking”, by Liv Lunde (1983)
6. “Avoidance of stress corrosion cracking (SCC) in cargo tanks, reliquefaction condensors and condensate return pipework with liquefied ammonia cargoes” by Society of International Gas Tanker and Terminal Operators LTD (1988).
7. National Transportation Safety Board, Hazardous material accident brief, accident no – DCA03MZ002 (2003).
8. “The Effect of Oxygen and Water on Stress Corrosion Cracking of Mild Steel in Liquid and Vaporous Ammonia”, by Liv Lunde and Rolf Nyborg, Plant/operations progress Vol.6, No. 1 (1987).
9. Examination report: Minnesota Department of Labor & Industry, Morris missile - Ammonia nurse tank explosion (June 6, 2005). http://www.doli.state.mn.us/nursetankexplosion.html